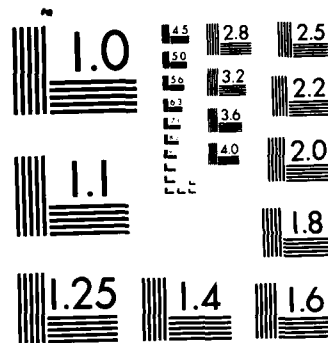MICROCOPY RESOLUTION TEST CHART

NATIONAL BUREAU OF STANDARDS-1963-A

Stochasticity of Particle Orbits in a Collective Particle Accelerator

AD-A162 418

G. GANGULI AND H. G. MITCHELL

Science Applications International Corporation
McLean, VA 22102

P. J. PALMADESSO

Geophysical and Plasma Dynamics Branch
Plasma Physics Division

December 6, 1985

DTIC FILE COPY

NAVAL RESEARCH LABORATORY
Washington, D.C.

85 1° 1° 038

REPORT DOCUMENTATION PAGE

1a. REPORT SECURITY CLASSIFICATION	1b. RESTRICTIVE MARKINGS
UNCLASSIFIED	AD-A162 418

2a. SECURITY CLASSIFICATION AUTHORITY	3. DISTRIBUTION/AVAILABILITY OF REPORT
	Approved for public release; distribution unlimited.
2b. DECLASSIFICATION/DOWNGRADING SCHEDULE	

4. PERFORMING ORGANIZATION REPORT NUMBER(S)	5. MONITORING ORGANIZATION REPORT NUMBER(S)
NRL Memorandum Report 5664	

6a. NAME OF PERFORMING ORGANIZATION	6b. OFFICE SYMBOL (If applicable)	7a. NAME OF MONITORING ORGANIZATION
Naval Research Laboratory	Code 4780	

6c. ADDRESS (City, State, and ZIP Code)	7b. ADDRESS (City, State, and ZIP Code)
Washington, DC 20375-5000	

8a. NAME OF FUNDING/SPONSORING ORGANIZATION	8b. OFFICE SYMBOL (If applicable)	9. PROCUREMENT INSTRUMENT IDENTIFICATION NUMBER
Office of Naval Research		

8c. ADDRESS (City, State, and ZIP Code)	10. SOURCE OF FUNDING NUMBERS			
	PROGRAM ELEMENT NO.	PROJECT NO.	TASK NO.	WORK UNIT ACCESSION NO.
Arlington, VA 22217	(See page ii)			

11. TITLE (Include Security Classification)

Stochasticity of Particle Orbits in a Collective Particle Accelerator

12. PERSONAL AUTHOR(S)
Ganguli, G.,* Mitchell, H.G.,* and Palmadesso, P.J.

13a. TYPE OF REPORT	13b. TIME COVERED	14. DATE OF REPORT (Year, Month, Day)	15. PAGE COUNT
Interim	FROM 9/84 TO 9/85	1985 December 6	24

16. SUPPLEMENTARY NOTATION   *Science Applications International Corporation, McLean, VA 22102

This research was sponsored by the Office of Naval Research.

17.	COSATI CODES		18. SUBJECT TERMS (Continue on reverse if necessary and identify by block number)
FIELD	GROUP	SUB-GROUP	Relativistic electron beam Stochasticity
			Collective accelerator

19. ABSTRACT (Continue on reverse if necessary and identify by block number)

A detailed investigation of the behavior of particle orbits in the simultaneous presence of three large amplitude waves such as those encountered in the Collective Particle Accelerator (CPA) experiment at the Naval Research Laboratory is undertaken. Stochasticity arising out of the resonance overlap of the waves can influence the particle dynamics significantly and thereby affect the outcome of the experimental results. Choice of initial phase and energy for successful operation is identified and discussed.

20. DISTRIBUTION/AVAILABILITY OF ABSTRACT	21. ABSTRACT SECURITY CLASSIFICATION
☒ UNCLASSIFIED/UNLIMITED ☐ SAME AS RPT ☐ DTIC USERS	UNCLASSIFIED

22a. NAME OF RESPONSIBLE INDIVIDUAL	22b. TELEPHONE (Include Area Code)	22c. OFFICE SYMBOL
P. J. Palmadesso	(202) 767-3630	Code 4780

DD FORM 1473, 84 MAR   83 APR edition may be used until exhausted.
All other editions are obsolete

10. SOURCE OF FUNDING NUMBERS

PROGRAM ELEMENT NO.	PROJECT NO.	TASK NO.	WORK UNIT ACCESSION NO.
61153N	RR011-07-0J RR011-09-01		DN480-607

CONTENTS

Dist | Special

A-1

iii

STOCHASTICITY OF PARTICLE ORBITS
IN A COLLECTIVE PARTICLE ACCELERATOR

I.   INTRODUCTION

High energy and high density beams have been of considerable interest in recent years. A novel method to achieve such a high density high energy particle beam was proposed by Friedman[1] in 1978 in a device called the Collective Particle Accelerator (CPA). Briefly, the device is a travelling wave accelerator with a novel feature: the travelling wave (T.W.) which does the accelerating is generated on the axis of a cylindrical drift tube as a consequence of the interaction between (1) a periodically bunched annular electron beam injected near the drift tube wall, and (2) a periodically rippled axial magnetic field. The advantage of this as compared to conventional travelling wave devices, in which the T.W. is a cavity mode, arises from the fact that the phase velocity in the CPA may be chosen to be as slow or fast as desired, within limits to be discussed below, and may be easily varied as a function of distance along the drift tube by varying the wavelength of the magnetic ripple. Thus ions may, in principle, be accelerated along the axis either coparallel or antiparallel to the motion of the annular beam, or electrons may be accelerated in the antiparallel direction. An important side effect of this method of generating the T.W. is the fact that three large amplitude waves are simultaneously generated in the device: a forward (i.e. coparallel with the annular beam velocity) T.W.; a backward T.W.; and a stationary wave pattern.

The first experiments in support of the CPA concept were conducted around 1976. A relativistic annular electron beam was propagated a distance of 7 meters, without bunching and with straight magnetic field lines. In the next phase the beam was bunched and again 7 meter propagation was achieved. Addition of the magnetic field ripple in the third stage of the effort was similarly successful. Next, a solid beam with current ~10% of the annular beam current was successfully propagated along the axis in the absence of the annular beam. The full experiment, solid beam plus bunched annular beam with rippled B field was then tried. The solid beam did not come out at the end opposite to which it was injected, and diagnosis of this beam through the annular beam was

difficult, so a simpler experiment was tried. A solid beam was injected into an annular beam without bunched or B field ripples, but was not detected near the other end, although a magnetic field disturbance attributed to the solid beam was detected close to the solid beam emitter. Note that without bunches and ripples no acceleration can take place, in which case the solid beam cannot overcome the potential hill near the annular beam cathode, so in the full experiment one does not expect the solid beam to hit the opposite end even if it propagated. A number of variations of these experiments were attempted in 1979; e.g., the solid beam was carried to a point well inside the drift tube via a smaller radius drift tube projecting inside the annular beam, but still the solid beam was not observed to propagate the remaining distance. Again we emphasize that observation of the weak solid beam through the strong annular beam is difficult, and the negative result in the unmodulated case cannot be regarded as definitive.

Various theoretical analyses for the stability properties of the dual beam system were undertaken in order to understand the experimental results. Chen and Palmadesso[2] studied the diocotron instability in the CPA in an attempt to understand the sensitivity to small misalignments of the annular beam encountered in the first experiment. The $\ell = 1$ diocotron mode can be excited by a shift of the annular beam axis off the drift tube axis, and was shown to have a growth length cmparable to the device length for the parameters used. The growth of the instability is not significant if the beam is very accurately centered initally, but is enough to cause the beam to hit the wall if the initial displacement is within an e-fold or two of the distance between the beam and the wall.

Uhm[3] showed that the transverse oscillation instability has a growth time ~ 1/5 of the beam transit time for the CPA parameters used. However, Ganguli and Palmadesso[4] used the wave kinetic equations in a finite length device to show that the transverse oscillation instability behaves like a backward convective instability in the rest frame of the solid beam i.e., in this frame the growth is spatial rather than temporal and vanishes at the beam head. The implication is that the front part of the beam (about 5 meters worth in this case) would make it across the device even though the tail end of the beam was being torn up as the head completed its transit.

2

Thus the theoretical models analyzed so far do not account for the failure of the solid beam to emerge from the end of device, in the case where an accelerating T.W. is present. These theoretical models did not investigate the role of the important second and third large amplitude waves generated and the influence of these waves on the particle dynamics. The purpose of this paper is to study the role of these waves in determining the particle dynamics of the CPA and hence influencing the experimental outcome. In section II we describe our theoretical model, provide the equation of motion governing the CPA system and describe the method of solution. In section III we give the results of the calculations and discuss the ramifications of these and finally in section IV we provide concluding remarks.

II. THEORY

As discussed earlier an important side effect of the way that the travelling waves are generated in the CPA is the simultaneous presence of three large amplitude waves in the device. It is well known that if a particle is under the influence of two or more waves with resonance widths broad enough to bridge (or nearly bridge) the gap between the wave phase velocities, then the multiple resonance can make the particle orbits stochastic[5]. With the onset of stochasticity the predictability of the particle motion is lost. This is a possible scenario taking place inside the CPA. The expression for the axial electric fields generated by the bunched beam and rippled B field is[1],

$$E_z(z, t) = - E_{zo}\left\{\cos\left[2\pi z\left(\frac{1}{\lambda} - \frac{1}{L}\right) - 2\pi ft\right]\right.$$

(1)

$$\left. - \cos\left[-2\pi z\left(\frac{1}{L} + \frac{1}{\lambda}\right) + 2\pi ft\right] - 2\sin\frac{2\pi z}{L}\right\},$$

where L is the wavelength of the rippled magnetic field, f and λ are the frequency and the wavelength of the modulation. $E_{zo} = (Q/4\epsilon_o)(r_1/r_oL)$ where r_o, r_1 are the equilibrium radius of the Annular Electron Beam (AEB) and the amplitude of the oscillations of the AEB due to the ripples of the magnetic field, and Q is charge/length. Equation (1) represents the superposition of a forward wave with a phase velocity given by,

3

$$v_{\phi f} = v \frac{L}{L + \lambda} , \tag{2}$$

where $v = f\lambda$, a backward wave with a phase velocity of

$$v_{\phi b} = - v \frac{L}{\lambda - L} , \tag{3}$$

and a stationary wave pattern.

Both travelling waves can accelerate ions but only the backward wave can accelerate the electrons since it can have a phase velocity approaching c (the velocity of light) which happens to be approximately the velocity of the electrons parallel to the magnetic field.

A particle subjected to the field given in (1) experiences the potential of both the forward and the backward waves along with the standing wave simultaneously. These are large amplitude waves whose resonance widths in velocity space scale as,

$$\frac{\Delta\omega}{k} = \frac{1}{k} \left(\frac{eE_{zo}k}{\gamma m_o} \right)^{1/2} \propto (\gamma m_o)^{-1/2} , \tag{4}$$

where $\Delta\omega$ is the resonance width in the frequency space, k is the wave number and $\gamma = (1 - v^2/c^2)^{-1/2}$. For the typical CPA parameters $(eE_{zo}k/m_o)^{1/2}/k \sim O(c)$; for low γ this implies an overlap of resonance leading to stochastic motion. As a consequence of the stochasticity in the orbits, the particles (electrons in our case) spend longer time inside the device thereby increasing the space charge and decreasing the value of the critical current. However, equation (4) also implies that for sufficiently large injection energy (initial value of γ) the resonance widths will be small enough so that stochastic motions will not occur. In view of the results of the CPA experiments we must investigate the role of stochasticity and estimate injection energy thresholds.

4

The equation of motion for the electrons in the CPA is given by,

$$\frac{dp}{dt} = -eE_z(z,t), \tag{5}$$

$$\frac{dz}{dt} = v(p) = \frac{1}{m_o}\frac{p}{\sqrt{1 + p^2/m_o^2 c^2}}, \tag{6}$$

where e is the magnitude of electronic charge and E_z given by (1) can be expressed as,

$$E_z = -4E_{zo}\sin(2\pi\alpha\zeta)\cos^2\{\pi(\zeta - \tau)\} \quad . \tag{7}$$

Here, $\zeta = z/\lambda$, $\alpha = \lambda/L$ and $\tau = ft + 1/4$. The equations of motion can be rewritten in dimensionless form as,

$$\frac{d\zeta}{d\tau} = \frac{\bar{p}}{\sqrt{1 + \bar{p}^2/\sigma^2}} \tag{8}$$

and

$$\frac{d\bar{p}}{d\tau} = (\frac{4eE_{zo}}{\lambda f^2 m_o})\sin(2\pi\alpha\zeta)\cos^2\{\pi(\zeta - \tau)\}, \tag{9}$$

where $\sigma = c/f\lambda$, $\bar{p} = p/f\lambda m_o$, m_o is the rest mass of the electrons.

We shall first study an infinitly long system by means of surface-of-section plots. After injecting a single particle at $\tau = 0$ we shall let the system represented by (8) and (9) run in time, and plot $\bar{p}$ and ζ for $\tau = 1,2,3....$ etc., given the initial momentum $\bar{p}_o$ and position ζ_o. We take $E_{zo} = 15$ MV/meters, $\alpha = 2$, $f = .995 \times 10^9$ Hz, and $\lambda = 0.3$ meter. These parameters are typical of the experiment[1]. Note that the system is periodic in ζ and hence we shall plot ζ modulo 1. The results will be

5

discussed in the following section.

After examining the infinite device to gain general insights we will study a finite device of 7 meters. Accumulation of electrons in the device is detrimental to its operation and may be caused by delays in time of flight. This enhances the electron density inside the device and decreases the critical current. In order to estimate the lag time of the electrons we plot,

$$S = \frac{\tau_t}{\tau_{min}} - 1, \tag{10}$$

as a function of time. Here τ_t is the transit time of the electrons through the device and $\tau_{min} = 7/c$ is the minimum time that the electron needs to travel the device of 7 meters when the electron velocity remains close to the speed of light c. Thus orbits with small S do not contribute to charge accumulation in the device while the higher values of S indicate highly distrubed electron orbits which contribute to an enhancement of the space charge cloud and a decrease in the limiting current.

Also, experimentally it is not possible to launch all the particles at the same phase initially. We shall study S as a function of $\Phi = -2\pi(\zeta_0 + \tau_0 - 1/4)$, the value at injection of the backward (accelerating) wave phase, for various injection energies γ_0. The results are discussed in the following section.

III. RESULTS AND DISCUSSION

We find two kinds of orbits exhibited on the surface of section plot. "Integrable" orbits are indicative of the existence of a well-behaved constant of the motion which confines the motion of the particle through phase space to a subspace of reduced dimension. The intersection of an integrable orbit with a two-dimensional surface of section such as that in Fig. 1 takes the form of a sequence of points $\left(\bar{p}(\tau_n), \zeta(\tau_n)\right)$ for $\tau_n = 0, 1, 2, \ldots,$ which lie on a simple one-dimensional curve or, in special cases, on a single "fixed" point. In general, the obvious global constants of the motion are exploited to reduce the dimension of the system of motion equations before one constructs a surface of section plot, so that the additional constants associated with integrable orbits exist only

6

in local regions of phase space, and it is rarely possible to express them analytically. Each of the nested closed curves near ζ mod 1 ~ .5, γ < 40 in figures 1 and 2 represents an integrable orbit corresponding to a different initial condition. At the center of this group of nested orbits is a fixed point, which corresponds to periodic motion passing through the stable force null of the backward wave at integer values of τ , i.e., the electron returns to the point ζ = .5 mod 1 at τ = 1,2,3,etc..

The four or five outermost curves which pass through ζ mod 1 = 0 with p $\leq$ -10 (i.e. $\gamma \geq$ 10) also represent distinct integrable orbits. No calculations were made in the blank regions at higher values of γ, but it is believed that all orbits in this region are integrable. At high energies the resonance widths of the three waves are small, the resonances are well separated, and solid beam electrons (v ~ -c) interact strongly only with the backward wave. The electron velocity exceeds the backward wave phase speed when γ > 10, so that an accelerated electron cannot maintain a constant phase relationship with the wave. Electrons gain energy, slip smoothly out of the phase interval in which the force due to the electric field is coparallel with the velocity, then decelerate while continuing to advance in phase. As the particle loses energy the resonances broaden. If the electron in this idealized infinite system has sufficient energy, it will slide forward in phase to the next accelerating region before its speed decreases to the point where it matches the phase speed of the backward T.W., and before resonance overlap occurs. The lowest energy integrable orbit of this group of orbits slows down until its speed is infinitesimally greater than the backward wave phase velocity at the point it reaches the unstable (hyperbolic) force null of the backward T.W. at $2\pi(\zeta+\tau)$ = 0 (ζ mod 1 = 0 on the surface of section plots); thus γ never falls below 10 on this orbit. There is also a set of integrable orbits representing high energy particles with positive velocities which are outside the resonaces of all three waves. These orbits are not physically meaningful for the CPA and will not be discussed further here.

"Stochastic" orbits occupy regions in which no such local well behaved constants of the motion exist, and these orbits meander through the entire phase space allowed by the global constants of the motion, with the restriction that they may not cross the "KAM" surfaces[6] (roughly speaking,

7

these are surfaces in phase space traced out by integrable orbits). In the 2-D surface of section plots, a single stochastic orbit accounts for all the points between the integrable regions discussed above. This orbit behaves in a chaotic manner at low energies (γ less than about 10), but catches the accelerating phase of the backward wave at random intervals and then gains energy in an orderly way. Segments of the stochastic orbit with γ above about 10 rise and fall in energy in much the same manner as the high-energy integrable orbits, but the electron speed falls below the backward T.W. phase speed ($\gamma \sim 10$) while the particle is still in the deceleration phase, so that the particle continues to lose speed and energy and slips in phase with respect to the backward T.W. at an increasing rate. Finally the motion ceases to be dominated by the backward T.W., and the particle falls back into the chaotic resonance overlap region below $\gamma \sim 10$.

A rough calculation of the electron orbits for $\gamma > 10$ may be performed by assuming that the particles have a constant velocity of $-c$ and are only affected by the backward wave, in which case the momentum equation takes the form

$$\frac{d\bar{p}}{d\tau} = (\frac{eE_{zo}}{\lambda f^2 m_o}) \cos [-2\pi(\zeta_o + (1-\sigma)\tau - 1/4]], \tag{11}$$

where ζ_o is the injection value of ζ. This equation may be solved to give an analytic expression for the energy γ of the particle as a function of the phase ϕ of the particle relative to the backward wave, the injection energy γ_o, and the injection phase Φ:

$$\gamma \sim \gamma_o + (\frac{eE_{zo}}{cfm_o}) \frac{1}{2\pi(\sigma-1)} (\sin(\Phi) - \sin(\phi)) \tag{12}$$

$$= \gamma_o + 280 (\sin(\Phi) - \sin(\phi))$$

where the CPA parameters have been used. An electron injected at the unstable force null ($\Phi = \pi/2$) at the speed of the backward wave ($\gamma_o = 10$) achieves its maximum energy at phase $\phi = -\pi/2$. This energy is $\gamma = 570$, which is in good agreement with Fig. 1 for the threshold energy above which all electrons have integrable orbits. In a finite length device, the electron stays with the backward wave only for a finite time and the phase

8

slippage is limited in size. Thus, not all particles below the threshold will become stochastic in a finite length device. For a device of length 7 meters, a particle traveling at the speed of light will remain in the device for 2.3×10^{-8} sec, which implies that $\Delta\tau \approx 23$ for this choice of the parameters f and λ, and that the maximum phase shift that the particle can undergo is $2\pi(1-\sigma)\Delta\tau \sim -\pi/4$. From equation (12), this means that, if $\gamma \geq 10 + 280\left(\sin(\pi/8) - \sin(-\pi/8)\right) \sim 224$, a particle cannot become stochastic in a 7 meter device with these parameters.

In figures 3a to 3g we display plots of the normalized lag time S against the injection phase of Φ of the backward wave for 7 different injection energies from $\gamma = 5$ to $\gamma = 250$. These plots are pertinent to a finite device of 7 meters. We learn two very important features of the CPA operation from this figure. First and foremost it is seen that as the injection energy γ increases from $\gamma = 5$ to $\gamma = 250$ the mean value of S decreases steadily. This implies that for high enough injection energies there is uniform motion no matter what the initial phase is. For lower energies the mean value of S increases significantly indicating that the electrons are spending longer times inside the device. This implies an electron space charge cloud build up inside the device and consequently a decrease in the limiting current. The value of the injection energy in the experiment for the solid beam was on the order of $\gamma = 5$, and hence it is not surprising to find the absence of the accelerated solid beam in the experiment, which was conducted with injected current very close to the critical current as traditionally calculated.

Along with the decrease in the mean value of S, we also notice a shrinkage of the interval $\Delta\Phi$ over which S is significant as the injection energy γ_0 is increased. If this interval of injection phases is avoided, then uniform motion could be achieved even at lower energies. For example, if $\gamma_0 = 5$ and $\Phi = \pi$, figure 3a shows no significant lag time. On the other hand even for high energy, say $\gamma = 150$, (figure 3e) if the initial phase is around zero we can expect stochastic behavior. As noted earlier we find that the optimum phase for acceleration is $\Phi = \pi$. Figure 3a indicates that particles launched with an injection phase $\Phi = \pi$ can be accelerated even for injection energies lower than the γ of the background wave since the particles cannot shift into the chaotic region before leaving the finite

9

device. When a uniformly solid beam is injected, particles of all phases will simultaneously occupy the drift tube. Thus the charge build up associated with the particles with phase in the stochastic range can be detrimental to successful acceleration of those particles which have the optimum phase.

IV. CONCLUSION

We have studied the influence of the three large amplitude waves that arise due to the CPA wave generation scheme on the particle dynamics in the CPA. For typical CPA parameters the resonance width of the waves are broad enough to overlap for low energy electrons. This gives rise to stochasticity in the particle orbits if the initial phase is not properly chosen. The stochasticity enhances the transit time of the electrons consequently giving rise to an electron cloud build up inside the device. The charge build up inside the device decreases the critical current and could prevent the propagation of the solid beam. Further, we conclude that in the CPA experiment those particles of the solid beam that were launched at the optimum phase must not have caused any problems. Since the beam was solid there was a continuous range of injection phases and the particles in the stochastic range contributed to the charge build-up in the device which in turn prevented propagation and acceleration of the optimum phase locked particles. To avoid these effects for a solid beam an injection $\gamma \geq 225$ is necessary. However, if the solid beam is injected in small pulses around the optimum phase it is possible to achieve successful acceleration even for low injection energies.

We have studied the lag time as a function of the phase of the backward wave. It seems that by properly choosing the injection phases (pulsed solid beam) it is possible to avoid the stochasticity and minimize the transit time.
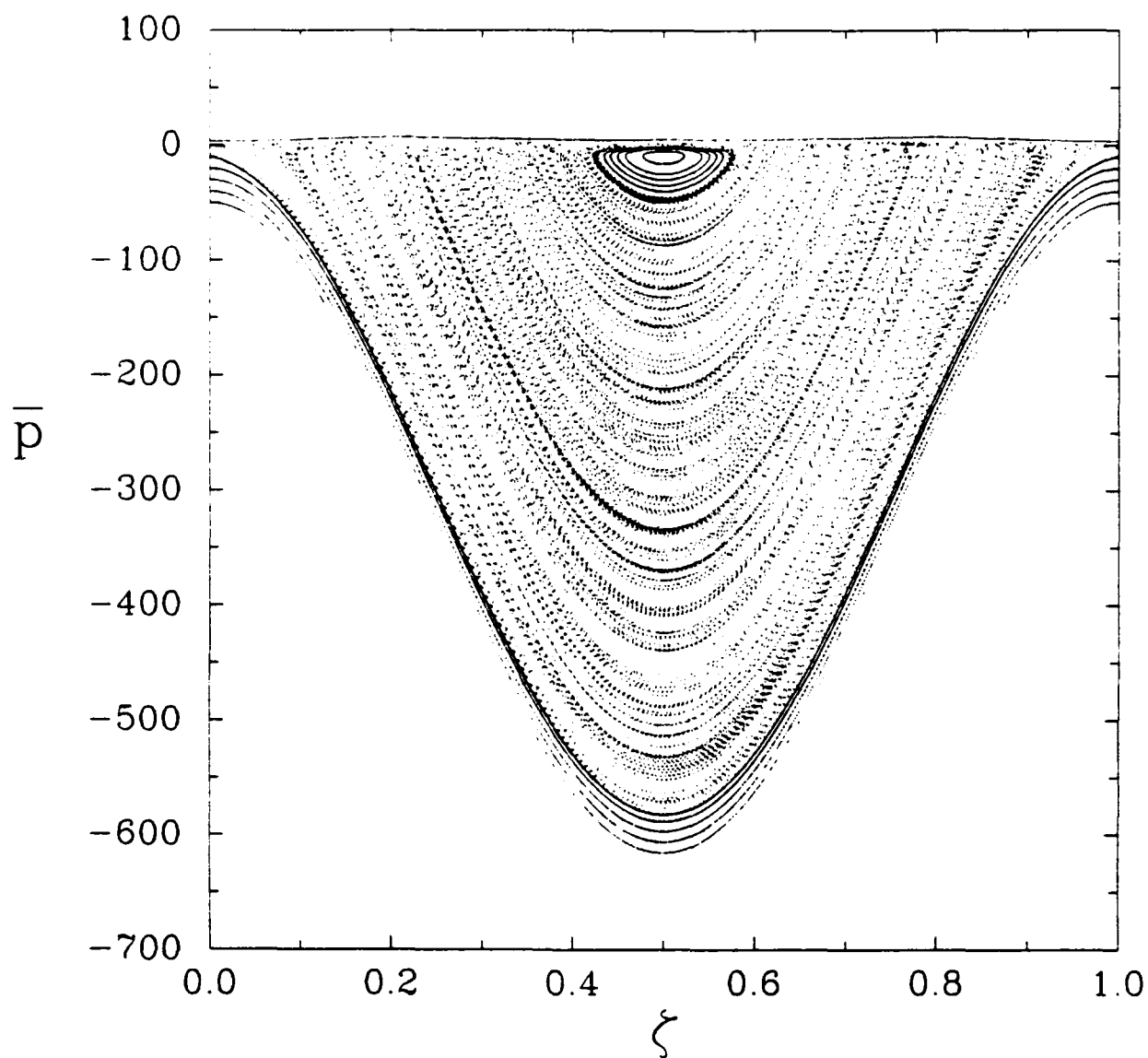
Fig. 1. Surface of section plot. Here E_{zo} = 15 Mv/ Meter, α = 2, λ = 0.3. The magnitude of the normalized momentum $\bar{p}$ is approximately equal to γ.
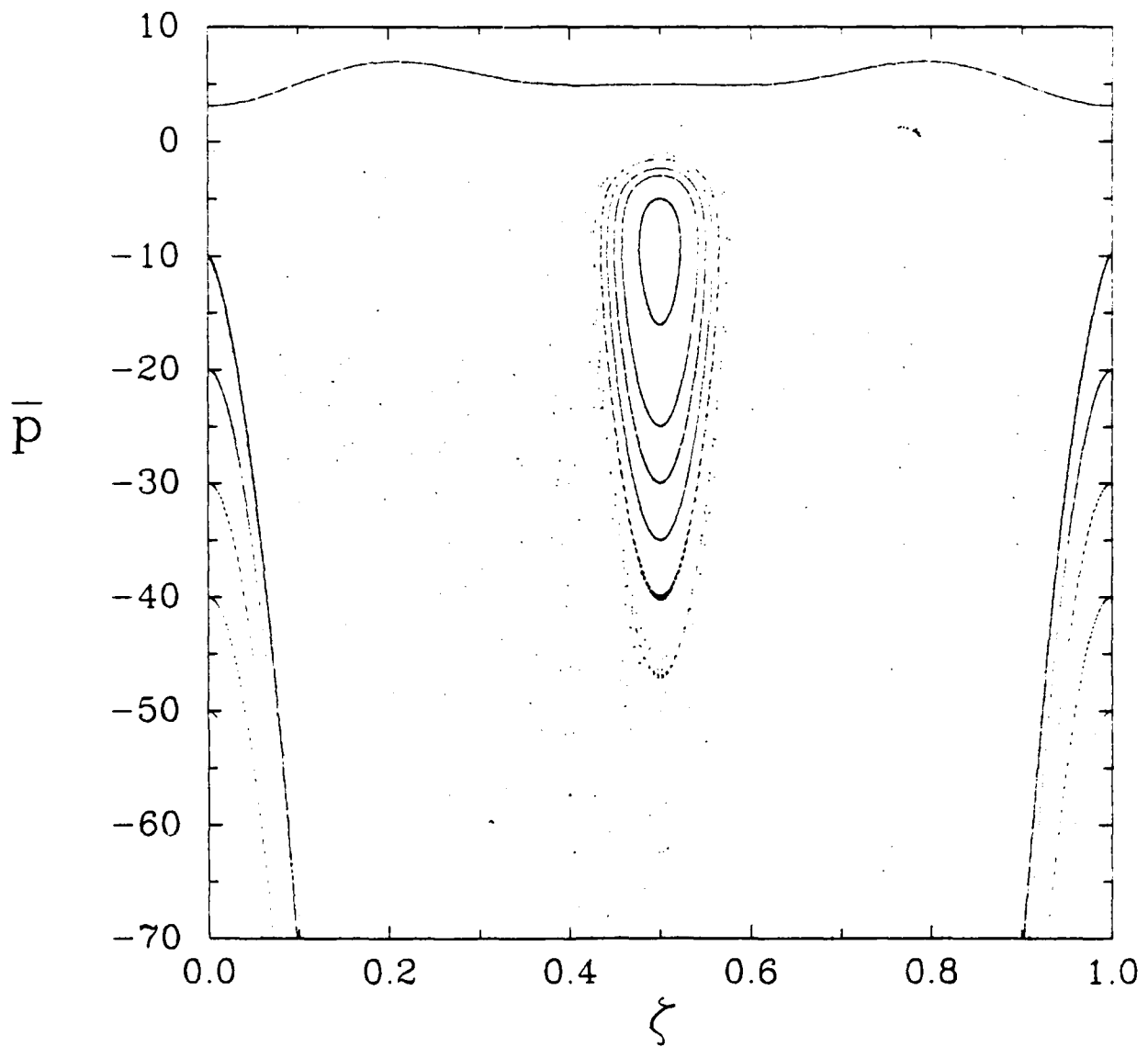
Fig. 2. An enlarged version of the low energy part of the stochasticity region of figure 1.
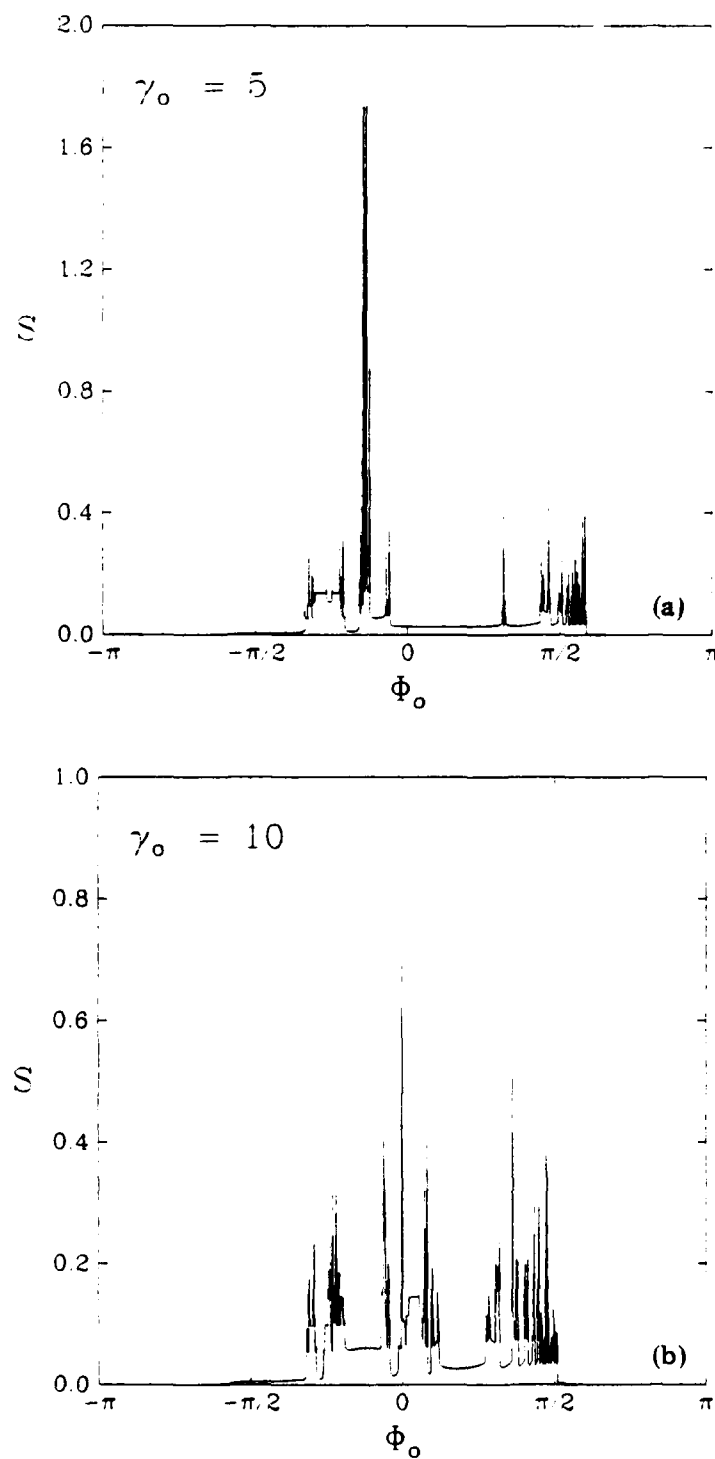
Fig. 3. A plot of the lag time S against the injection phase Φ of the backward wave for a device of 7 meters. The initial values of Y at injection are:

(a) Y = 5, (b) Y = 10, (c) Y = 15, (d) Y = 50, (e) Y = 150, (f) Y = 200 , and (g) Y = 250.

Fig. 3. Cont'd. A plot of the lag time S against the injection phase Φ_o of the backward wave for a device of 7 meters. The values of γ_o at injection are:

(a) $\gamma_o = 5$, (b) $\gamma_o = 10$, (c) $\gamma_o = 15$, (d) $\gamma_o = 50$, (e) $\gamma_o = 150$, (f) $\gamma_o = 200$, and (g) $\gamma_o = 250$.
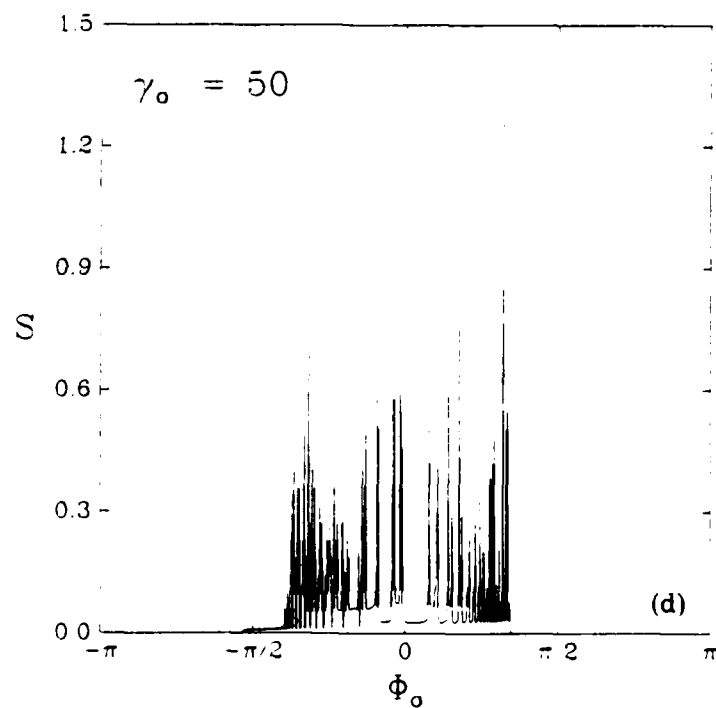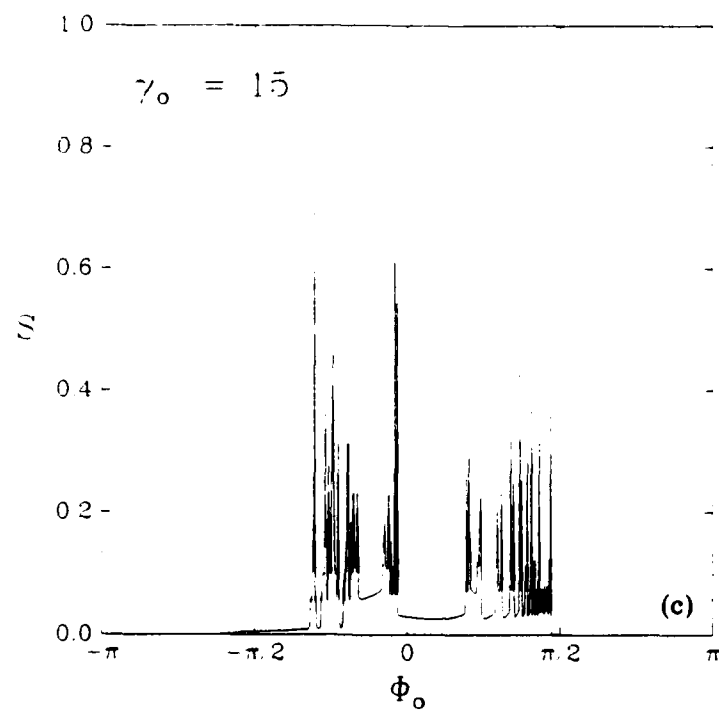
14

Fig. 3. Cont'd. A plot of the lag time S against the injection phase Φ_o of the backward wave for a device of 7 meters. The values of Υ_o at injection are:

(a) $\Upsilon_o = 5$, (b) $\Upsilon_o = 10$, (c) $\Upsilon_o = 15$, (d) $\Upsilon_o = 50$,

(e) $\Upsilon_o = 150$, (f) $\Upsilon_o = 200$, and (g) $\Upsilon_o = 250$.

15

Fig. 3. Cont'd. A plot of the lag time S against the injection phase Φ_0 of the backward wave for a device of 7 meters. The values of γ_0 at injection are:

(a) $\gamma_0 = 5$, (b) $\gamma_0 = 10$, (c) $\gamma_0 = 15$, (d) $\gamma_0 = 50$,

(e) $\gamma_0 = 150$, (f) $\gamma_0 = 200$, and (g) $\gamma_0 = 250$.
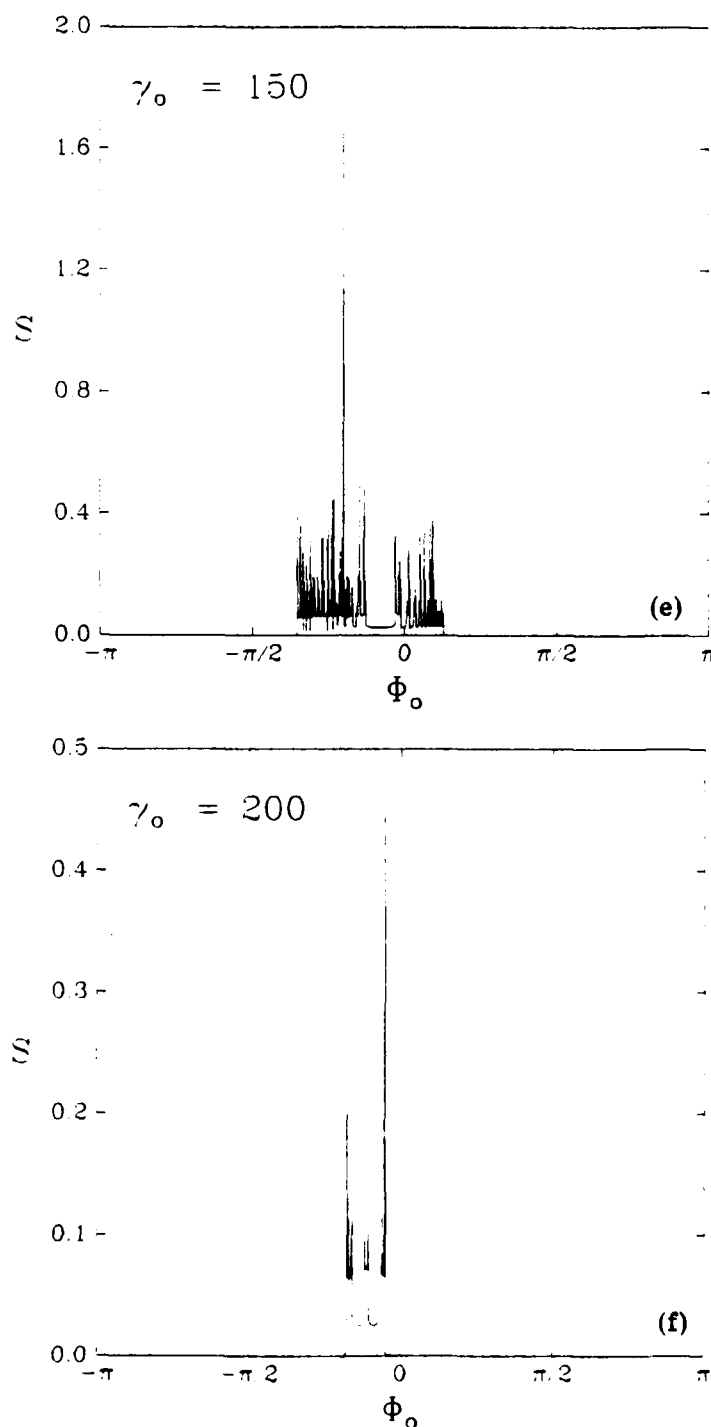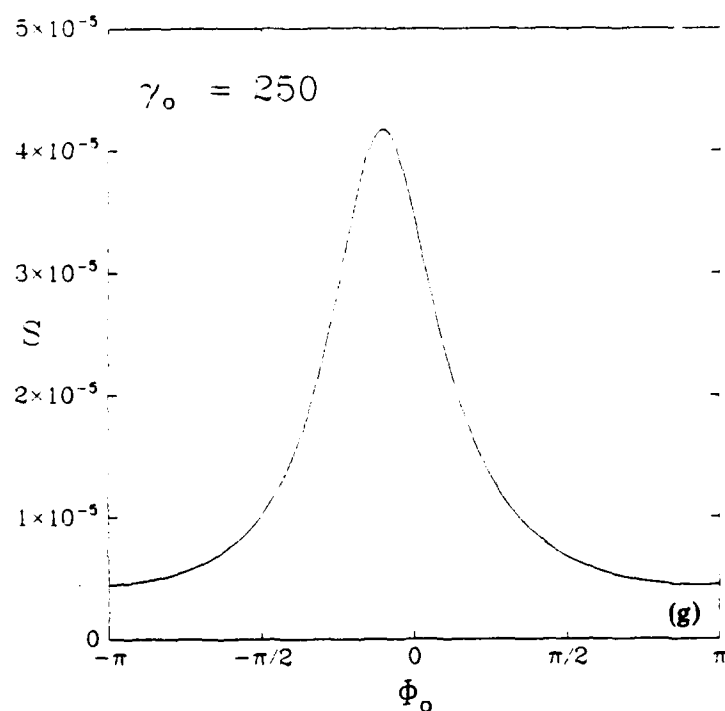
16

REFERENCES

1.   M. Friedman, NRL Memorandum Report No. 3724, (1978).

2.   R. Chen and P. Palmadesso, Phys. Fluids, $\underline{24}$, 357 (1981).

3.   H.S. Uhm, Phys. Fluids $\underline{25}$, 1908 (1982).

4.   G. Ganguli and P. Palmadesso, J. Appl. Phys., $\underline{55}$ 2715 (1984).

5.   B.V. Chirikov, Plasma Physics, 1, 253 (1960).

6.   H.G. Shuster, _Deterministic Chaos: An Introduction_, Weinheim:Physik-Verlag (1984).

DISTRIBUTION LIST

Naval Research Laboratory
Washington, DC 20375-5000
    Attn: Director of Research, Code 1001
          Dr. S.L. Ossakow, Code 4700
            (26 copies)
          Dr. J.D. Huba, Code 4780
            (50 copies)
          Dr. P. Palmadesso, Code 4700.1P
          Dr. I.M. Vitkovitsky, Code 4701
          Dr. A. Robson, Code 4760
          Dr. P. Sprangle, Code 4790
          Dr. M. Lampe, Code 4790
          Dr. M. Friedman, Code 4700.1
          Dr. A. Ali, Code 4700.1
          Dr. J.R. Grieg, 4763
          Dr. J.B. Aviles, Code 6650
          Dr. I. Haber, Code 4790
          Dr. R. Hubbard, Code 4790
          Dr. D. Colombant, Code 4790
          Code 2628 - 20 copies
          Code 1220 - 1 copy

Office of Naval Research
Department of the Navy
Arlington, VA 22217
    Attn: Dr. C.W. Roberson, Code 412
          Dr. W.J. Condell, Code 412

Air Force Weapons Laboratory
Kirtland Air Force Base
Albuquerque, NM 87117
    Attn: Lt. Col. J.H. Havey

Commander
Naval Sea Systems Command
Department of the Navy
Washington, D.C. 20363
    Attn: NAVSEA 03H (Dr. C.F. Sharn)

U.S. Army Ballistic Research Laboratory
Aberdeen Proving Ground, MD 21005
    Attn: Dr. D. Eccleshall (DRXBR-BM)

Ballistic Missile Defense Advanced
    Technology Center
P.O. Box 1500
Huntsville, AL 35807
    Attn: Dr. L. Harvard (BMDSATC-1)

B-K Dynamics, Inc.
15825 Shady Grove Road
Rockville, MD 20850
    Attn: Mr. T. Kuhn

Intelecom Rad Tech
P.O. Box 81087
San Diego, CA 92138
    Attn: Mr. W. Selph

Lawrence Livermore Laboratory
University of California
Livermore, CA 94550
    Attn: Dr. R.J. Briggs
          Dr. Kelvin Neil
          Dr. T. Fessenden
          Dr. E.P. Lee

Mission Research Corporation
735 State Street
Santa Barbara, CA 93102
    Attn: Dr. C. Longmire
          Dr. N. Carron

National Bureau of Standards
Gaithersburg, MD 20760
    Attn: Dr. Mark Wilson
          Dr. S. Penner

Science Applications Intl. Corp.
1200 Prospect Street
LaJolla, CA 92037
    Attn: Dr. M.P. Fricke
          Dr. W.A. Woolson

Science Applications Intl. Corp.
5150 El Camino Road
Los Altos, CA 94022
    Attn: Dr. R.R. Johnston
          Dr. Leon Feinstein

Science Applications Intl. Corp.
McLean, VA 22102
    Attn: Mr. W. Chadsey
          Dr. A. Drobot

Science Applications Intl. Corp.
8201 Capwell Drive
Oakland, CA 94621
    Attn: Dr. J.E. Reaugh

19

Naval Surface Weapons Center
White Oak Laboratory
Silver Spring, MD 20903-5000
 Attn: Mr. R.J. Biegalski
   Dr. R. Cawley
   Dr. J.W. Forbes
   Dr. C.M. Huddleston
   Dr. G.E. Hudson
   Mr. G.J. Peters
   Mr. N.E. Scofield
   Dr. E.C. Whitman
   Dr. M.H. Cha
   Dr. H.S. Uhm
   Dr. R. Fiorito

C.S. Draper Laboratories
Cambridge, MA 02139
 Attn: Dr. E. Olsson
   Dr. L. Matson

M.I.T. Laboratories
P.O. Box 73
Lexington, MA 02173
 Attn: Dr. J. Salah

Physical Dynamics, Inc.
P.O. Box 1883
La Jolla, CA 92038
 Attn: Dr. K. Brueckner

Avco Everett Research Laboratory
2385 Revere Beack Pkwy.
Everett, MA 02149
 Attn: Dr. R. Patrick

Defense Documentation Center (2 copies)
Cameron Station
5010 Duke Street
Alexandria, VA 22314
 Attn: TC

Defense Advanced Research Projects Agency
1400 Wilson Blvd.
Arlington, VA 22209
 Attn: Dr. Shen Shey

JAYCOR
205 S. Whiting St.
Alexandria, VA 22304
 Attn: Dr. J. Guillory

Physics International, Inc.
2700 Merced Street
San Leandro, CA
 Attn: Dr. S. Putnam
   Dr. E. Goldman

Mission Research Corporation
1720 Randolph Road, SE
Albuquerque, NM 87106
 Attn: Dr. Brendan Godfrey

Princeton University
Plasma Physics Laboratory
Princeton, NJ 08540
 Attn: Dr. Francis Perkins, Jr.

McDonnell Douglas Research Laboratories
Dept. 223, Bldg. 33, Level 45
Box 516
St. Louis, MO 63166
 Attn: Dr. Michael Greenspan

Cornell University
Ithaca, NY 14853
 Attn: Prof. David Hammer
   Prof. Ravi Sudan

Sandia Laboratories
Albuquerque, NM 87185
 Attn: Dr. Bruce Miller
   Dr. Barbara Epstein
   Dr. T. Lockner

University of California
Physics Department
Irvine, CA 92717
 Attn: Dr. Gregory Benford
   Dr. Norman Rostoker

Massachusettes Institute of Technology
Cambridge, MA 02139
 Attn: Prof. R. Davidson
   Prof. G. Bekefi

Ian Smith, Inc.
3115 Gibbons Drive
Alameda, CA 94501
 Attn: I. Smith

Lawrence Berkeley Laboratory
Berkeley, CA 94720
 Attn: D. Keefe
   A. Faltens

Lockheed Palo Alto Research
 Laboratory
Palo Alto, CA 94304
 Attn: Dr. J. Siambis

Director of Research
U.S. Naval Academy
Annapolis, MD 21402 (2 copies)

END

FILMED

2-86

DTIC